Acta Chemica Scandinavica, 1997: 51: 24–30
Printed in UK – all rights reserved

ACTA
CHEMICA SCANDINAVICA
ISSN 0904–213X

Defect Structure and Molecular Dynamics of Doped Ice and Natural Snow

Hans Christian Gran,† Eddy Walther Hansen‡ and Bjørn Pedersen*

Department of Chemistry, University of Oslo, Box 1033 Blindern, N-0315 Oslo, Norway

Gran, H. C., Hansen, E. W. and Pedersen, B., 1997. Defect Structure and Molecular Dynamics of Doped Ice and Natural Snow. – Acta Chem. Scand. 51: 24–30. © Acta Chemica Scandinavica 1997.

Ice doped with from 1 to 1000 ppm HCl, HBr, HI, NaCl or $NaNO_3$ has been studied with ^{1}H-NMR methods. The spectrum consists in general of a small narrow peak superposed on a broader peak. The linewidth and the spin–lattice relaxation time of the broad peak (from the solid part of the ice samples) have been determined as a function of temperature from about −90 °C to the melting point. The temperature dependence indicates that the dopants create defects in ice different from the intrinsic defects in pure hexagonal ice as the observed activation energies, from 20 to 30 kJ mol^{-1}, are significantly smaller than the activation energy observed for pure ice (ca. 60 kJ mol^{-1}). We have not succeeded in observing a liquid phase in pure ice, and therefore conclude that any liquid phase reported in 'pure' ice must be due to impurities. Also, samples of natural snow have been studied. The experimental results show that the bulk of the snow gets purer as the snow anneals on the ground.

The ideal structure of ordinary (hexagonal) ice is well known, but much less exact knowledge is available on its defect stucture and dynamics. It was found early on that the structure of ice was similar to the high-temperature form of tridymite.[1] In this form of tridymite the silicon atoms are tetrahedrally bound to four oxygen atoms. Each oxygen atom is situated midway between two silicon atoms. In hexagonal ice, the stable form of ice under a pressure of 1 atm, the oxygen atoms are situated in the positions of the silicon atoms. In early X-ray diffraction studies the hydrogen atoms could not be located. Bernal and Fowler[2] proposed that (1) every oxygen is covalently bound to two hydrogen atoms and (2) there is one (and only one) hydrogen atom located between two neighboring oxygen atoms. These so-called Bernal–Fowler rules were strongly supported by Pauling's famous calculation of the residual entropy of ice.[3] Pauling regarded ice as a disordered structure of hydrogen-bonded water molecules in which the geometry of the water molecules is only slightly different from the geometry found for the molecule in the gas phase (Pauling's 1935 values, still valid: O–H ≈95 pm and <H–O–H ≈105°). In Pauling's model of ice each water molecule can be located in six different orientations, and he assumed that the energy differences between the orientations are too small to order the molecules at low temperature. The Pauling model was confirmed by the neutron diffraction study of ice by Peterson and Levy.[4] These authors claimed that the H–O–H angle is close to tetrahedral (109.5°). Chidambaram[5] has shown that it is not possible to say from the neutron diffraction data of Peterson and Levy that the H–O–H angle is significantly different from the value found for the unbound water molecule (104.5°), which is preferred from bond-energy and spectroscopic considerations. This is supported by a more recent neutron diffraction study by Kuhs and Lehmann.[6]

Bloembergen *et al.*[7] studied ice in their pioneering paper on nuclear magnetic relaxation and ascribed the observed relaxation times (T_1 and T_2) to hindered rotation of the H_2O molecules. The first extensive study of pure and doped ice (KOH) with CW NMR methods was done by Kume,[8] and by pulse NMR methods by Barnaal and Lowe[9] on pure ice and on HF-doped ice by Barnaal *et al.*[10] HF is the dopant most commonly used. This is because HF is isoelectronic with the water molecule, and it has been assumed that HF substitutes a water molecule in the ice lattice, creating one vacant O–O bond.[11] We will argue, however, that very likely the HF molecule is ionized in ice as it is in dilute water solutions. Experimental results, to be presented in this paper, show that the dopants used (HCl, HBr, HI, NaCl or $NaNO_3$) introduce other defects in the ice lattice than the intrinsic defects present in pure ice, making it possible for some of the water molecules to reorient more freely.

† Present adress: NBI, PO Box 123, Blindern, N-0314 Oslo, Norway.
‡ Present adress: SINTEF Oslo, PO Box 124, Blindern, N-0314 Oslo, Norway.
* To whom correspondence should be addressed.

We have studied pure and doped ice and natural snow by measuring the temperature variation of the ^{1}H NMR spectrum and the spin–lattice relaxation time (T_1).[12] The ^{1}H spectrum of doped ice and natural snow consists in general of a small narrow peak superposed on a broader peak, showing that a small part of the ice samples is liquid. The dependence on temperature and dopant concentration of the liquid phase (the narrow peak) in HCl-doped ice has been published earlier by Hansen.[13] Clifford[14] and Kvlividze *et al.*[15] claim that also the spectrum of pure ice contains a narrow peak due to a liquid phase. We have therefore looked for a narrow peak in the NMR spectra of pure ice with a large surface-to-bulk ratio. We will concentrate in this paper on the broad peak from the solid part of the samples. In solid salt hydrates it has been found that the dominating relaxation mechanism is dipolar relaxation from uncorrelated, temperature-activated 180° flips of the water molecules.[16] Slotfeldt–Ellingsen and Pedersen[17] showed that this relaxation mechanism is not efficient enough to relax the proton spin system in ice. However, it has recently been found that reorientation between all six allowed orientations for each water molecule in ice is probably the process relaxing the proton spin system.[18,19]

We have studied natural snow in search of a molecular explanation of why the very first melt water in the spring may have concentrations of pollutants about 5–10 times the values found in bulk snow.[20] As T_1 is very susceptible to impurities in the ice lattice we wanted to see if NMR could discriminate between impurities located on the surface of the snow or distributed in the ice lattice.

Experimental

The ^{1}H NMR spectra were recorded at 60 MHz on a Varian dual-purpose NMR spectrometer. A representative spectrum is given in Fig. 1. The linewidth reported below is the linewidth between the inflection points of the broad peak recorded at low modulation amplitude. T_1 was measured at 8.00 MHz on a home-built pulse spectrometer using a series of 90° pulses. The uncertainty in the T_1-measurements is 5–10%. The uncertainty in the temperature is ± 0.3 K.

Preparation of pure and doped ice samples. The water was deionized and distilled, and stoichiometric amounts of the various dopants were added (1.0–1000 ppm mol fraction). The sample tubes (diameter 5 mm, wall thickness 0.4 mm) were cleaned with chrome sulfuric acid, rinsed with distilled water and kept in distilled water at least 1 wk before use. The water samples were quenched in liquid nitrogen for about 90 s.

The samples of natural snow. Five sets of samples of natural snow were taken from the end of March to the beginning of May 1979. The samples were taken from a location at Gran, Hadeland from an open, horizontal field of about 80 m^2 far from roads and industry. The samples were taken from four levels in the snow and brought to the laboratory in polyethylene bottles and stored in dry ice [CO_2(s)]. In the bottles the snow changed to crusted snow. T_1 was measured at -56 °C. pH and electrical conductivity were also measured after the samples were melted.

Results

Experimental T_1 data are given as a function of temperature in Figs. 2–6. The correlation times calculated from the experimental linewidths as a function of temperature for pure ice and HCl-doped ice are given in Fig. 7. In Fig. 8 all T_1 data are plotted as a function of the linewidth of the corresponding spectra. As the linewidths were not recorded at exactly the same temperature as

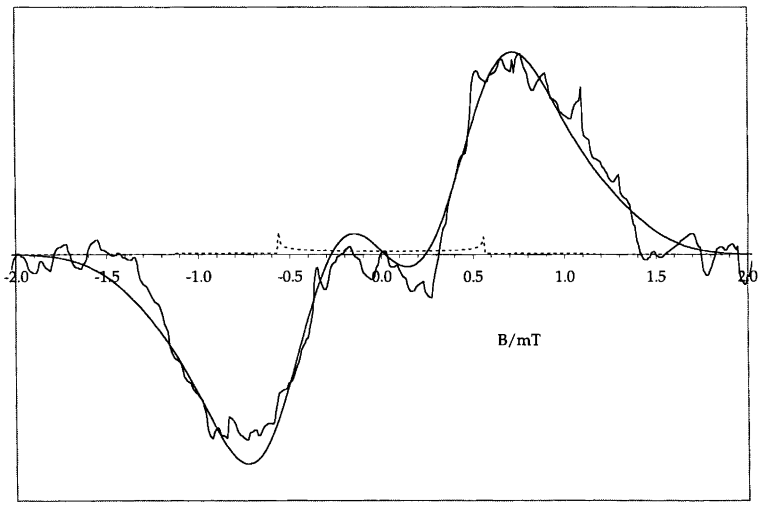

Fig. 1. The observed ^{1}H spectrum of polycrystalline ice at -29.4 °C. The smooth line is the calculated pair spectrum fitted visually to the observed spectrum. The broken line shows the spectrum of an isolated pair averaged over all orientations (the Pake spectrum).

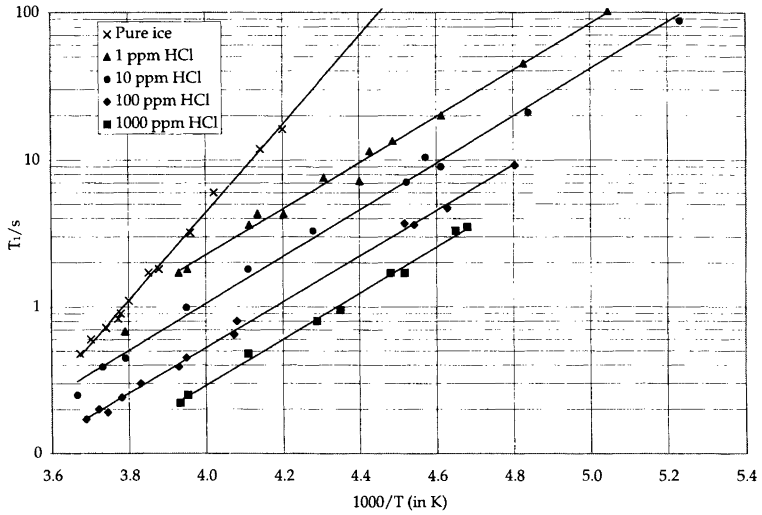

Fig. 2. Experimental spin–lattice relaxation times (T_1) for pure ice and HCl doped ice plotted vs. inverse absolute temperature. The solid lines are fitted to the observed data by the method of least squares.

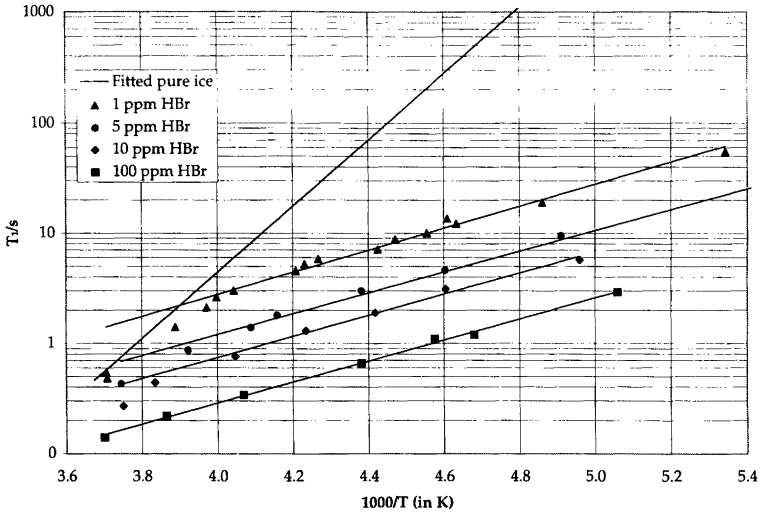

Fig. 3. Experimental spin–lattice relaxation times (T_1) for HBr doped ice plotted vs. inverse absolute temperature. The solid lines are fitted to the observed data by the method of least squares.

T_1, the linewidth at each T_1 temperature was determined by interpolation.

T_1 is determined by the molecular motion, and the T_1 graphs show that we are on the low-temperature side of a T_1 minimum. T_1 is therefore proportional to $\omega_0{}^2\tau$, where ω_0 is the resonance frequency and τ the correlation time characterizing the motion.[21] We furthermore assume that the temperature dependence of the correlation time is given by the familiar Arrhenius equation: $1/\tau = P\exp[-\Delta E/(RT)]$, where P is the pre-exponential factor (the attempt frequency), ΔE the activation energy and T the absolute temperature.[17] Hence, log T_1 plotted vs. $1/T$ is expected to give a straight line with slope equal to $\Delta E/R$.

Pure ice. The importance of working with pure samples has been stressed by workers in the field.[10] As will be discussed below, our linewidth and T_1 data on pure ice are in agreement with earlier reports. We have specifically looked for a narrow peak from a liquid phase. We made a sample containing small Teflon spheres to get a large surface-to-volume ratio, but we were unable to detect a narrow peak.

The ^{1}H-NMR spectrum of polycrystalline pure ice at low temperature (Fig. 1) shows signs of fine structure, corresponding to a so-called Pake doublet, as expected for a solid where the protons are situated in pairs with the intrapair distance (ca. 160 pm) shorter than the shortest interpair distances (ca. 230 pm).[22] The smooth curve also shown in Fig. 1 is a calculated pair spectrum fitted visually to the observed spectrum.[23] When the spectrum starts to narrow at about $-30\,^\circ$C the fine structure disappears and the line-shape becomes approximately Gaussian. Above about $-6\,^\circ$C (to the melting point) the line-shape becomes more Lorentzian, as expected when the spectrum is motionally narrowed.

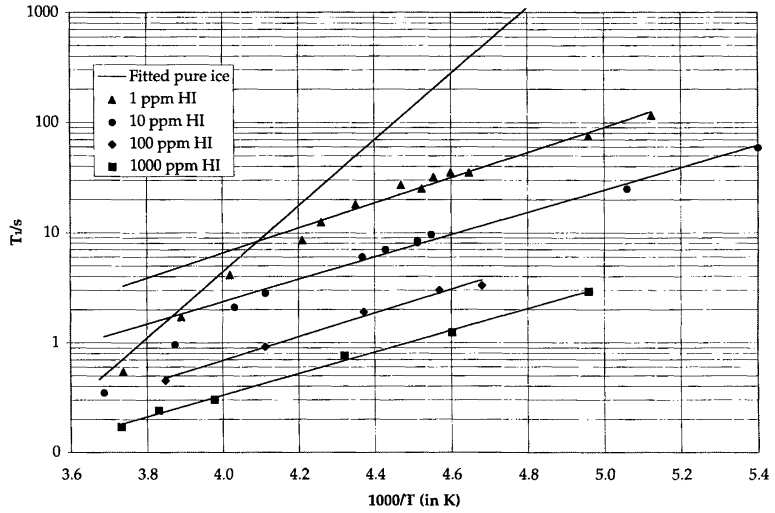

Fig. 4. Experimental spin–lattice relaxation times (T_1) for HI doped ice plotted vs. inverse absolute temperature. The solid lines are fitted to the observed data by the method of least squares.

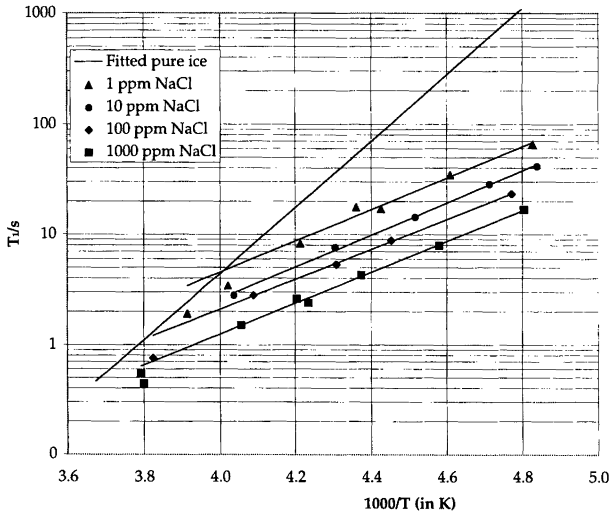

Fig. 5. Experimental spin–lattice relaxation times (T_1) for NaCl doped ice plotted as the function of inverse temperature. The solid lines are fitted to the observed data by the method of least squares.

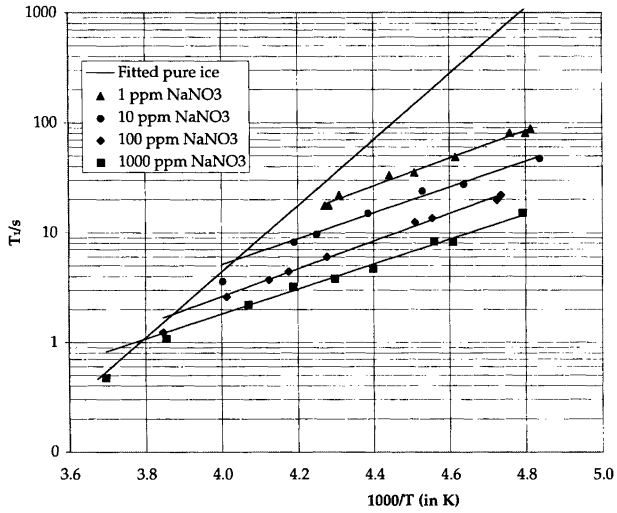

Fig. 6. Experimental spin–lattice relaxation times (T_1) for $NaNO_3$ doped ice plotted vs. inverse absolute temperature. The solid lines are fitted to the observed data by the method of least squares.

As pointed out above, T_1 increases proportionally to the square of the resonance frequency. At $-30\,^{\circ}C$ $T_1 \approx 10$ s, hence T_1 is expected to be about 9 min at 60 Mhz and 100 min at 200 Mhz. It was therefore necessary to do the T_1 measurements at low frequency.

Doped ice. The T_1 data are given in Figs. 2–6 and the derived activation energies in Table 1. We see that the activation energy depends on the dopant, but not on the dopant concentration within the experimental uncertainty of ca. ± 1 kJ mol^{-1}. The values found for log $T_1(0)$ are also given in Table 1. A graph of log $T_1(0)$ vs. log [X] shows that log $T_1(0)$ decreases linearly with the inverse third root of the dopant concentration within the experimental uncertainty, i.e. the relaxation rate increases when the distance between the dopant ions becomes smaller.

In the region above $-30\,^{\circ}C$ we have calculated the correlation time (τ) from the Kubo–Tomita equation:[24]

$$\tau = \frac{16 \ln 2}{\gamma \Delta B} \operatorname{tg}\left[\frac{\pi}{2}\left(\frac{\Delta B}{\Delta B_0}\right)^2\right] \qquad (1)$$

Here ΔB is the linewidth and ΔB_0 ($=1.71$ mT) the constant linewidth below $-30\,^{\circ}C$. In Fig. 7 the derived values of the correlation time are plotted as a function of inverse temperature for pure and HCl-doped ice. We see that the experimental points determine straight lines. From the slope of the line, fitted with the method of least squares, we find $P = 1.0 \times 10^{15}$ Hz and $\Delta E = 59.8$ kJ mol^{-1} for pure ice. The value found for the

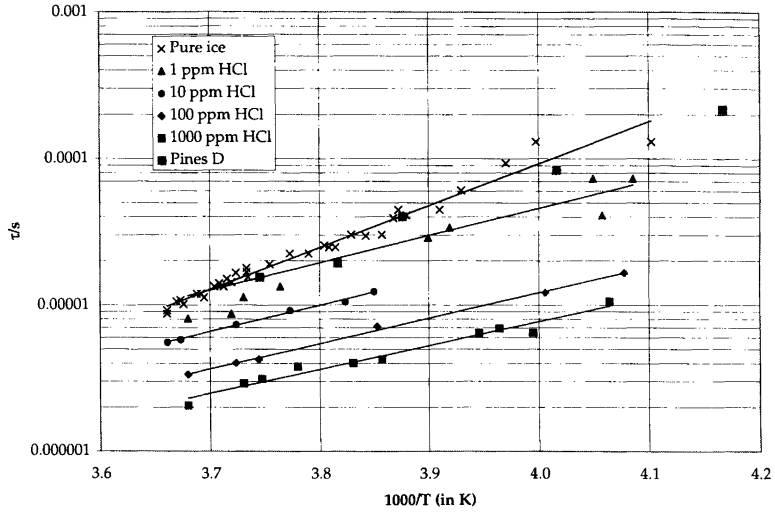

Fig. 7. The correlation times for pure ice and HCl-doped ice calculated from the experimental line widths using eqn. (1) plotted vs. inverse absolute temperature. The solid lines are fitted to the observed data by the method of least squares. In the figure are also included data from Ref. 19.

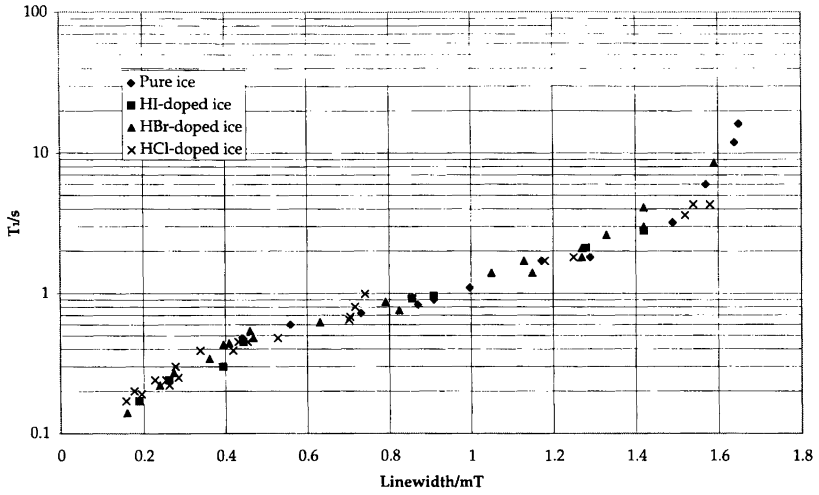

Fig. 8. Experimental spin–lattice relaxation times (T_1 logaritmic scale) plotted as function of the linewidth.

Table 1. Derived values for the activation energy (in kJ mol^{-1})/log $T_1(0)$[a] in doped ice from T_1 data (for pure ice: 59.8/−8.29)

[Dopant] (ppm)	HCl	HBr	HI	NaCl	$NaNO_3$
1	30.1/−5.93	19.2/−3.57	21.9/−3.75	27.3/−5.05	24.2/−4.13
5		18.1/−3.70			
10	30.5/−6.35	18.3/−3.96	19.5/−3.69	27.9/−5.41	22.6/−4.00
100	29.8/−6.51	18.3/−4.37	20.6/−4.46	26.0/−5.11	24.2/−4.63
1000	30.1/−6.83		18.9/−4.42	26.8/−5.51	21.7/−4.28
Mean value	30.1	18.5	20.2	27.0	23.2

[a] log $T_1(0)$ = log T_1 at $1000/T = 0$.

activation energy is not significantly different from the value found for T_1 (Table 1). Also the values found for HCl-doped ices agree within the experimental uncertainty with the values determined from the T_1 data in Fig. 2. (The mean activation energy obtained from the data in Fig. 7 is 34 kJ mol^{-1} compared to 30.1 kJ mol^{-1} given in Table 1.) The experimental uncertainty for the values determined from the dependence of the linewidth versus inverse temperature is greater than the experimental uncertainty for the corresponding values derived from the T_1 data. This is mainly due to the much smaller temperature region where the linewidth changes significantly (from 0 to −30 °C). We conclude that the narrowing of the broad peak is due to the same process

determining T_1. Also, linewidths determined from the other doped samples show similar correlations and they are therefore not presented.

By comparing the correlation time calculated from the linewidth of pure ice at 250 K and T_1at the same temperature we find that $T_1 = 4.74 \times 10^4\ \tau$.

Natural snow. T_1 increased from about 10 s to about 70 s in the snow samples taken closest to the surface as shown in Fig. 9. T_1 in pure ice is about 310 s at the temperature (−56 °C) in which these measurements were made. Compared to T_1 found for the doped samples this suggests that the snow was fairly pure and underwent an annealing process from the end of March to the beginning of May. Some of the samples were refrozen after being melted in the same way as the doped ice samples were made. Surprisingly, T_1 was then found to be longer than in the snow. This shows that T_1 is not only a function of the impurity content, but also depends on the distribution of the impurities in the snow, surface area, morphology and other factors.

Discussion

The calculated pair spectrum shown in Fig. 1 depends on the value of two parameters: the intrapair dipole–dipole coupling α [$=3\,\mu/(2R^3)$ with $\mu = 1.4104$ pm^3 kT] and the interpair coupling β. The shape of the spectrum depends only on β/α.[23] We find $\alpha = 0.565$ mT and $\beta = 0.271$ mT ($\beta/\alpha = 0.48$). The second moment of such a pair-powder spectrum is $(4/5)\alpha^2 + \beta^2 = 0.329$ mT^2. The second moment has been found earlier to be 0.32 (2) mT^2.[9a] From the obtained value of α we calculate the H–H distance in the water molecules in ice to be $R = 155$ pm, which is close to the value found by neutron diffraction 157 pm.[6] However, the distance is an average over the vibratory motion, and a correction for the molecular vibrations will affect this NMR distance and the neutron diffraction value differently. We regard the fit between the calculated spectrum and the observed spectrum in Fig. 1 as satisfactory. However, Barnaal and Lowe[9a] analyzed the FID from single ice crystals and polycrystalline ice in terms of the Pake model, and concluded that the calculated FID is not in satisfactory agreement with the observed FID within their experimental uncertainty.

The activation energy found for pure ice in this work (60 ± 1 kJ mol^{-1}) is equal to the value found by Barnaal and Lowe (59.0 ± 0.4 kJ mol^{-1}) in their very careful study.[9] The correlation times derived from the observed linewidths in this work are also in good agreement with the correlation times found by Pines *et al.*[19] from an analysis of the change in the ^{2}H-NMR lineshape versus temperature.

By comparing the correlation time calculated from the linewidth of pure ice at 250 K and T_1 at the same temperature we found that $T_1 = 4.74 \times 10^4\ \tau$. This is somewhat smaller than calculated by Barnaal and Lowe:[9] $T_1 = 1.37 \times 10^5\ \tau$ (corrected for the difference in resonance frequency) assuming H_2O jumps between 6 tetrahedral sites ignoring coupling to more distant molecules. If the couplings to more distant molecules are included in the Barnaal and Lowe calculation the calculated value will be smaller and closer to what we observe.

We were unable to detect a narrow peak from a liquid phase in pure ice even in samples with a large surface obtained by adding Teflon spheres to the water before freezing. In doped ice a narrow peak could be seen close to the melting points even when the concentration of dopant was as small as 1 ppm. The presence of a narrow peak in the ^{1}H NMR spectrum of 'pure' ice close to the melting point, reported by other workers,[14,15] suggests to us that the ice still contains impurities.

Our doped samples are not in thermodynamic equilib-

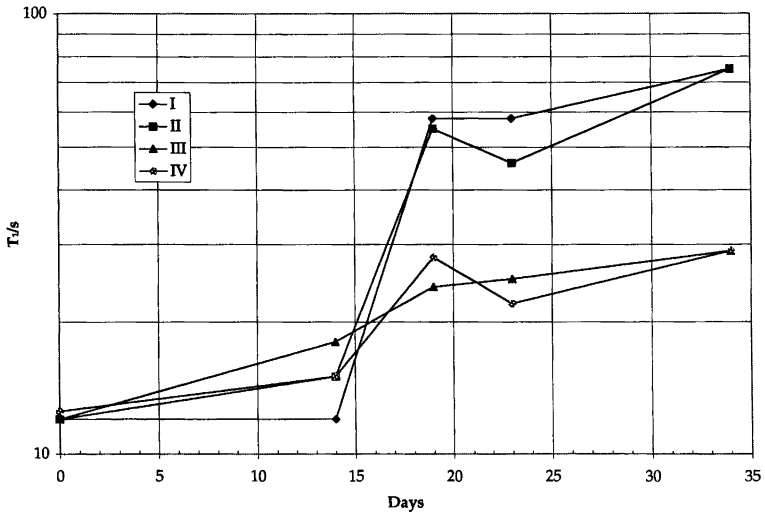

Fig. 9. Experimental spin–lattice relaxation times (T_1) for natural snow plotted as the function of time at the ground. The samples have been taken from different levels in the snow with I closest to the surface.

rium. The detailed study of the narrow peak in the ^1H spectra of HCl-doped ice[13] shows that the samples are probably frozen so fast that the dopant is trapped at the same sites as in the liquid before freezing. The strong acids and salts are expected to be ionized completely at these low concentrations.

Barnaal and Slotfeldt-Ellingsen[25] have shown that doped samples change when stored. After a couple of days the samples seem to stabilize, but when stored at $-20\,^{\circ}C$ for several years T_1 changes significantly. The recovery of the magnetization is not longer purely exponential in NaOH-doped ice indicating that the samples are no longer homogenous.[26] This can be due to annealing, reactions with the container or the atmosphere or other processes. We have concentrated on studying fairly fresh samples, hoping the impurities to be trapped in the positions they had in the liquid phase before freezing. Within experimental uncertainty the recovery of the z-magnetization is found to be exponential.

The molecular traffic in ice has been discussed in the literature on the basis of several possible defects: (1) the Bjerrum L-and D-defects i.e. either no H-atom on an O–O bond (L) or two H-atoms on an O–O bond (D); (2) ionic defects; in particular H_3O^+ ions and OH^- ions; (3) Schottky (water molecule vacancies) or Frenkel (water molecules in interstitial sites) defects.[18] In pure ice the tetrahedral jumps could be due to Bjerrum defects. It is reasonable to expect that defects created by doping are directly related to the ionic dopants. Doping with acids introduce H_3O^+ ions and anions in the lattice, and doping with salts will generate defects created by cations and anions. It is expected that the geometry of these defects will partly be determined by the ice structure and partly by energy gains created by small geometrical changes causing the ions to obtain a bonding situation similar to that observed in crystalline hydrates. In crystalline hydrates the dominating relaxation mechanism is 180° flips of the water molecules. Close to impurity ions the activation energy for 180° flips could be reduced. Also, hindered rotation of the H_3O^+ ions might contribute to the relaxation. The structure of $HX{\cdot}nH_2O$ with X=Cl and Br and $n=1$, 2, 3, 4 (only Br) have been determined by Lundgren and Olovsson;[27] unfortunately, however, nothing is known about the molecular motion in these hydrates which have not been studied by NMR.

We are in the long correlation time region, and therefore the ^1H spin system will relax with a common spin temperature. So even though some of the water molecules close to a defect may reorient faster than others, and therefore be more efficient in relaxing the spins, the whole spin system will relax exponentially back to equilibrium.[21]

Figure 8 shows a correlation between the observed linewidth and T_1, which is independent of dopant concentration. A similar correlation has been observed in HF-doped ice by Barnaal *et al.*[10] One should think that this somewhat surprising correlation implies that the basic process responsible for the relaxation is the same in pure and doped ice. However, as pointed out by Barnaal *et al.*,[10] it could also simply show that the correlation times for different processes are approximately equal.

References

1. Barnes, W. H. *Proc. R. Soc. London, Ser. A125* (1929) 670.
2. Bernal, J. D. and Fowler, R. H. *J. Chem. Phys. 1* (1933) 515.
3. Pauling, L. *J. Am. Chem. Soc. 57* (1935) 2680.
4. Petersen, S. W. and Levy, H. A. *Acta Crystallogr. 10* (1957) 70.
5. Chidambaram, R. *Acta Crystallogr. 14* (1961) 467.
6. Kuhs, W. F. and Lehmann, M. S. *J. Phys., Colloq.* (1987) C1-3/C1-8.
7. Bloembergen, N., Purcell, E. M. and Pound, R. V. *Phys. Rev. 73* (1948) 679.
8. Kume, K. *J. Phys. Soc. Jpn. 15* (1960) 1493.
9. (a) Barnaal, D. E. and Lowe, I. J. *J. Chem. Phys. 46* (1967) 4800. (b) *J. Chem. Phys. 48* (1968) 4614.
10. Barnaal, D., Kopp, M. and Lowe, I. J. *J. Chem. Phys. 65* (1976) 5495.
11. Gränicher, H. *Phys. Kondens. Mater. 1* (1963) 1.
12. Gran, H. C., Hansen, E. W., Pedersen, B. and Seip, H. M. *Abstracts of the VI International Symposium on the Pysics and Chemistry of Ice*, Rolla, MI, 1982.
13. Hansen, E. W. *J. Chem. Eng. Data 33* (1988) 99.
14. Clifford, *J. Chem. Soc. Chem. Commun.* (1967) 880.
15. Kvlividze, V. I., Kiselev, V. F., Kurzaev, A. B. and Ushakova, L. A. *Surf. Sci. 44* (1974) 60.
16. Holcomb, D. F. and Pedersen, B. *J. Chem. Phys. 36* (1962) 3270.
17. Slotfeldt-Ellingsen, D. and Pedersen, B. *Phys. Chem. Solids 38* (1977) 65.
18. Fujara, F., Wefing, S. and Kuhs, W. F. *J. Chem. Phys. 88* (1988) 6801.
19. Wittebort, R. J., Usha, M. G., Ruben, D. J. Wemmer, D. E. and Pines, A. *J. Am. Chem. Soc. 110* (1988) 5668.
20. Johannessen, M. and Henriksen, A. *Water Res. 14* (1978) 615.
21. See e.g. Slichter, C. P. *Principles of Magnetic Resonance*, 3rd edn., Springer, Berlin 1990.
22. Pake, G. E. *J. Chem. Phys. 16* (1948) 327.
23. Pedersen, B. *Acta Chem. Scand. 22* (1968) 444.
24. (a) Kubo, R. and Tomita, K. *J. Phys. Soc. Jpn. 9* (1954) 888. (b) Waugh, J. S. and Fedin, E. I. *Sov. Phys. Solid State 4* (1963) 1633. (c) Resing, H. A. *J. Chem. Phys. 43* (1965) 669.
25. Barnaal, D. and Slotfeldt-Ellingsen, D. *J. Phys. Chem. 87* (1983) 4321.
26. Barnaal, D. *Personal communication.*
27. *Lundgren, J.-O., Olovsson, I. In Schuster, P., Zundel, G., Sandorfy, C. Eds., The Hydrogen Bond*, North Holland, New York 1976, Vol II, Chapt. 10, pp. 470–526.

Received February 9, 1996.